

A Novel UHF RFID Slot Coupled Metallic Tag Antenna for Steel-Bar Applications

Jung Nam Lee*, Heon Kook Kweon, and Kwang Chun Lee

Abstract—In this paper, we propose a novel UHF RFID coupled slot metallic tag antenna with a radome. The proposed tag antenna consists of a frequency tuning slot, imaginary part tuning slot, real part tuning stub, micro-chip, and radome. The RFID tag antenna was designed and fabricated for use in the Korean and Japanese UHF band of 916.7 to 923.5 MHz. The measured 3 dB frequency bandwidth is 914 to 926 MHz. The measured read range is 11.5 m on a metallic surface. Details of the proposed tag antenna design, as well as simulated and measured results are presented and discussed.

1. INTRODUCTION

An RFID system is made up of a reader and a tag, and a UHF RFID system operates in the 902 to 928 MHz band in North America, 865 to 867 MHz band in Europe, 916.7 to 923.5 MHz band in Japan and 917 to 923.5 MHz band in Korea. RFID systems can be classified according to their frequency: low frequency, 125 to 134 kHz; high frequency, 13.56 MHz; UHF, 860 to 960 MHz; and microwave frequency, 2.4 and 5.8 GHz. The UHF and microwave RFID systems use the propagation of electromagnetic waves to transfer information between the tag and reader. If the object attaching the tag is positioned in the read zone of the reader, the reader transmits interrogation to the tag. The tag is responded to the interrogation of the reader. The UHF RFID system, tags are powered by a continuous wave signal transmitted by a reader, and a backscatter transmission from the reader is used to send back the data. A RFID applications have been categorized into supply chain, production, and others. Supply chain application are a recent development. A RFID based location identification system to facilitate easy and quick localization of vehicles on a shipping yard of an automotive assembly plant [1]. The RFID system is used for effective tire management with the objective of reducing operating costs [2]. The RFID systems have helped reduce the inventory holding costs and improve the inventory turnover at a LCD manufacturing company [3]. The RFID of the production reduce lead times and inventory holding costs, and improve throughputs. The RFID used a real-time management system for containers and improve container utilizations [4]. It has found application in the medical [5], parking management [6], and transportation [7]. Presently, tag antennas need to be placed on a metallic surface (container, vehicle, aircraft, and computer) in the supply chain and production. When typical label tags are placed on a metallic surface, they do not work efficiently. RFID tag antennas on metallic surfaces change the boundary condition, radiation pattern, efficiency, input impedance, gain, read range, and resonant frequency. To solve this problem, many researchers have developed other RFID antennas, including on metallic surface such as a wideband RFID tag antenna for metallic surfaces [8], orthogonally proximity-coupled patch antenna for a passive RFID tag on metallic surfaces [9], a RFID tag antenna for metallic surfaces using lossy substrate [10], a h-shaped tag antenna using microstrip feed design on metallic objects [11], loop antenna with interdigital coupled section on metallic objects [12], a UHF RFID/GPS fractal antenna for logistics management [13], a metallic RFID tag design for steel-bar and wire-rod management application in the steel industry [14], small proximity coupled ceramic patch antenna for

Received 11 October 2013, Accepted 6 December 2013, Scheduled 11 December 2013

* Corresponding author: Jung Nam Lee (jnlee77@gmail.com).

The authors are with the B4G Mobile Communications Research Department, Electronics and Telecommunications Research Institute, 161, Gajeong-Dong, Yuseong-Gu, Daejeon 305-350, Korea.

rectangular copper sheet, which is placed over the substrate. The tag antenna is filled with PET and polycarbonate in the area under the copper patch. The bottom of the tag antenna is placed on a steel-bar type metallic object. The operating frequency of the antenna can be controlled using a semi-circle slot length. The input impedance can be easily controlled by varying the F_S and F_L lengths. The proposed tag antenna has been designed and implemented for a micro-tag chip with an impedance of $Z_c = 30.2 - j212 \Omega$ at 920 MHz (Higgs-3 flip chip, operating frequency = 860–960 MHz, and sensitivity during read = -18 dBm). The optimal parameters are $L = 90$ mm, $W = 25$ mm, $F_S = 44.4$ mm, $F_L = 45$ mm, $F_W = 4$ mm, $F_D = 1$ mm, $C_L = 7$ mm, and $C_H = 0.5$ mm, with slot widths of 0.5 mm and 0.4 mm based on an optimization using Ansys High Frequency Structure Simulator (HFSS ver. 10) [18].

When RFID tag antenna is mounted on metallic objects, metallic surface can negatively affect the performance of a tag antenna in terms of resonant frequency and radiation efficiency. The resonant frequency and radiation pattern of the tag antenna changes, and its radiation efficiency decreases when the tag antenna is located on metallic objects. Therefore, the tag antenna is designed by approximately 3–5 mm separate from the metallic surface. The most of metallic tag antennas uses the air space, dielectric substrate, and form for this separate space. When the structure uses the air space, the size of the tag antenna is large, and the strength of the tag antenna is weak. Radiation efficiency is reduced due to high loss tangent when FR-4 used antenna structure. Dielectric substrate with a high permittivity can reduce the size of the metallic tag antenna [19]. However, the reading distance is decreased because of the dielectric loss. Therefore, most metallic tag antennas use foam instead of a dielectric. However, foam has a weak durability and is easily deformed by heat. Instead of foam, the proposed tag antenna uses polycarbonate, the heat and durability of which are strong.

3. MEASURED AND SIMULATED RESULTS

Figure 2 shows the measured results of the proposed tag antenna with and without radome. The proposed tag antenna was measured by attaching a steel-bar of 35 mm diameter and 200 mm length. A tag antenna was measured using an Anritsu Vector Network Analyzer (37397C) in an anechoic chamber.

Figure 2(a) shows the measured return loss of the proposed metallic tag antenna. The measured half-power bandwidth (return loss below 3 dB) is 1.3% from 914 to 926 MHz, which covers the 6.8 MHz bandwidth requirement of Korea and Japan for UHF RFID (916.7–923.5 MHz). It is clear that there is no distinguishable difference in return loss with and without steel-bar.

The proposed tag antenna was used for Alien microchip having the chip impedance of $Z_c = 27 - j200 \Omega$ at 920 MHz. However, we need a true chip impedance in which the chip is mounted in the antenna pad. The proposed tag antenna mounts the tag chip by the flip-chip bonding method in the antenna pad. As to this method, the electrical feature changes according to the bonding process and type of the adhesive. This causes the mismatch loss between the antenna and microchip. We

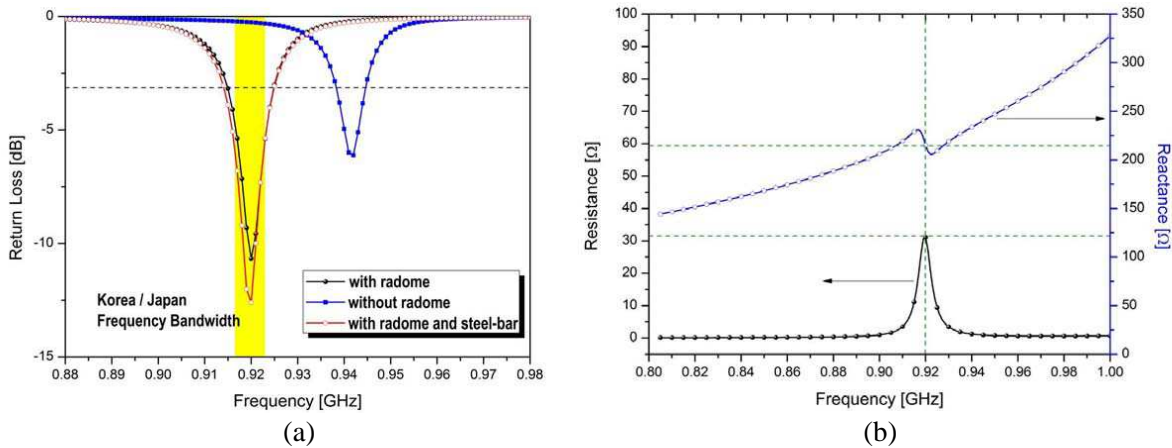


Figure 2. Measured results of the tag antenna: (a) return loss and (b) impedance responses.

tested a microchip directly using a standard $50\ \Omega$ probe or connector. The tag chip was soldered to a standard $50\ \Omega$ SMA connector assembly. The chip-connector assembly was connected to an RFID tester. The minimum power level of the chip was measured using the Alien reader with variable output power and frequency. The chip-connector assembly was then connected to a vector network analyzer whose output power was set to the minimum power level. The vector network analyzer whose output power is set to minimum power level measures the complex impedance and S_{11} and calculate threshold power sensitivity of the tag chip [20]. The measured tag chip impedance is $Z_c = 30.2 - j212\ \Omega$. The impedance responses of the tag antenna and of the measured chip (Higgs-3) are shown in Figure 2(b). The conjugate impedance of a measured tag chip (Higgs-3) is also shown in Figure 2(b). The resistance ($30.2\ \Omega$) and reactance ($212\ \Omega$) of the tag antenna has a similar value to the tag chip in the operating frequency.

Figure 3 shows the measured and simulated return losses of the proposed metallic tag antenna for different sizes of C_H , C_L , and radome heights. From Figure 3(a), we can see that as C_H is increased, the resonance frequency is moved to a lower frequency. Because a tag antenna should be able to change its minimum structure without changing the entire tag antenna structure, the frequency should be allowed to move easily. Figure 3(b) shows the effect of the frequency-tuning semi-circle slot width (C_L) on the return loss. The change of C_L width has small effect on the operating frequency.

The effects of the radome height on the return loss are shown in Figure 3(c). Except at the lowest height of 5 mm, the radome obtained similar results at 8.5 mm and over. Because the distance between the metallic radiator and radome is slight, when its height was 5 mm, the radiation feature was affected

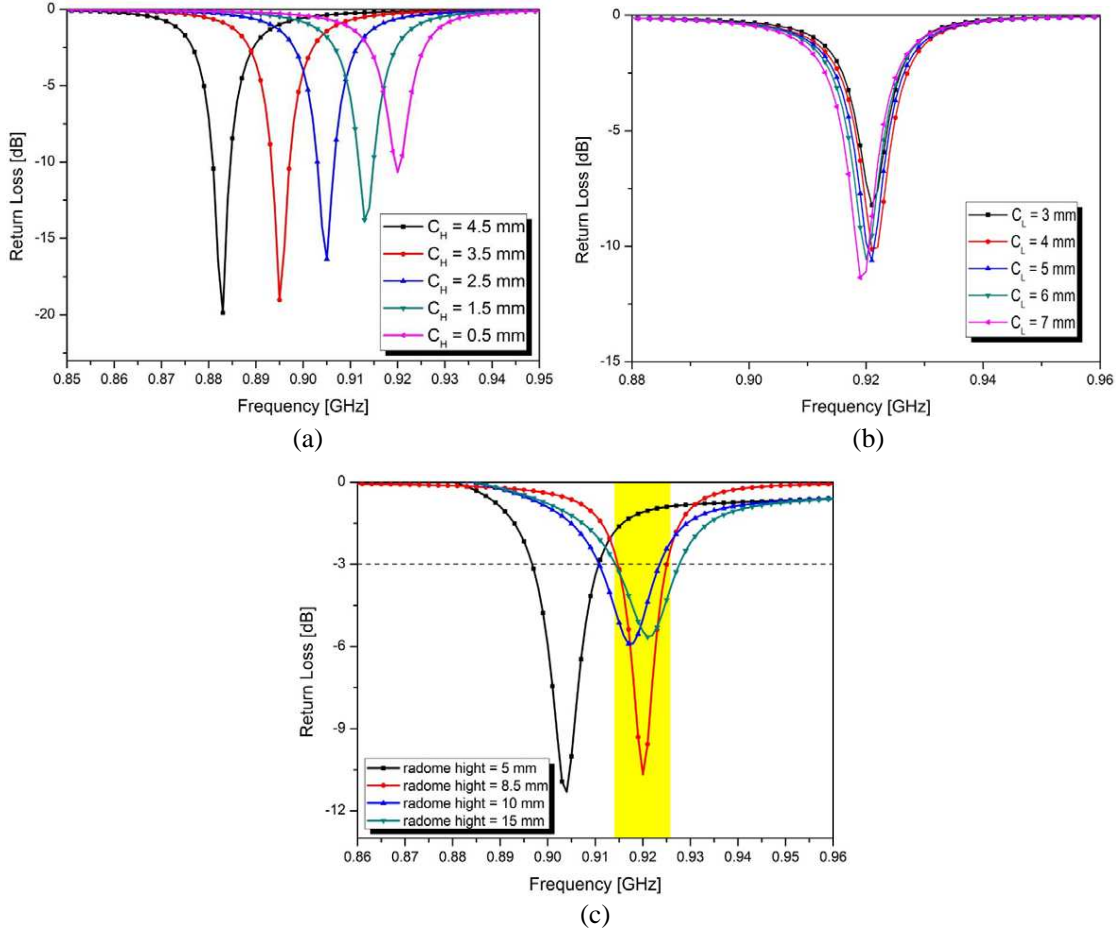


Figure 3. Simulated return loss of the tag antenna for (a) different sizes of C_H , (b) different sizes of C_L , and (c) radome heights.

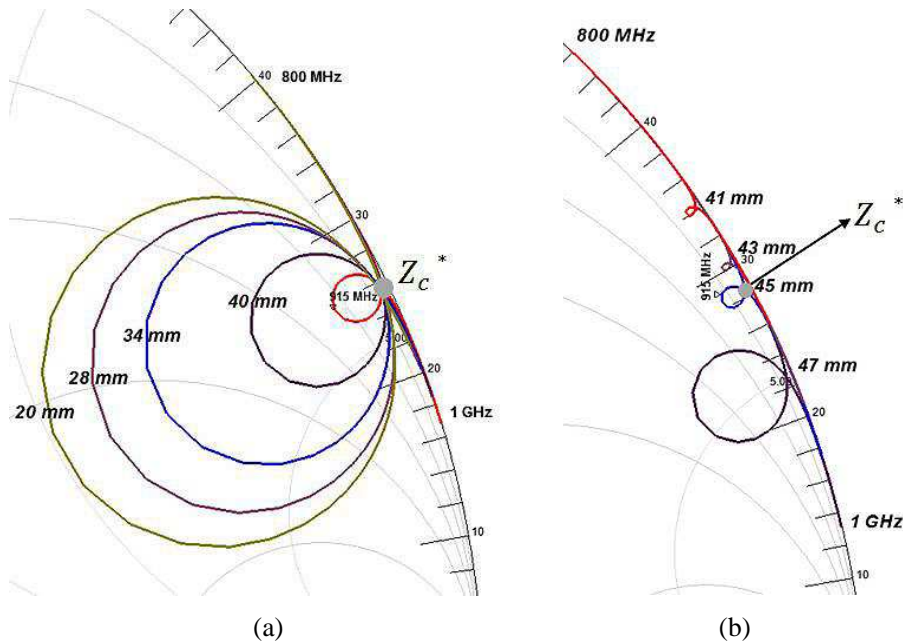


Figure 4. Input impedance feature of the tag antenna as a function of F_S and F_L : (a) F_S and (b) F_L .

by the radome and the operating frequency moved to a lower frequency. The optimized value for C_H , C_L , and the radome height for this design are 0.5 mm, 7 mm, and 8.5 mm, respectively.

Figure 4 shows the simulated input impedance of the proposed tag antenna. The impedance locus on the Smith chart exhibits an α -shaped feature around the complex conjugate value of Z_C [1]. To transmit the maximum power between a metallic tag antenna and a micro-chip, the tag antenna mostly uses a conjugate matching technique. The input impedance of the tag antenna $Z_a = R_a + jX_a$ depends on the self-reactance of the slot lengths F_S and F_L . The input resistance R_a of the tag antenna has a simple dependence on the coupled slot length F_S . The resistance of the tag antenna on the coupled slot length F_S is uniform along the coupled slot length. The total resistance can be easily controlled by varying the coupled slot length (F_S). As the coupled slot length decreases, the diameter of the impedance locus increases, as shown in Figure 4(a).

The input reactance X_a of the tag antenna is related to the self-inductance of the feed slot length (F_L). The total reactance can be easily controlled by varying the feed slot length (F_L). As the feed slot length decreases, the impedance locus is moved clockwise as shown in Figure 4(b).

Figure 5 shows the simulated E and H field distribution at 920 MHz. It is observed that the field direction is mainly horizontal plane (Y -axis). Thus, the polarization of the antenna can be expected to be linear polarized along horizontal plane (Y -axis). We can expect that the input impedance can be controlled by using the slot length (F_L and F_S) because the field distribution is intensive at the vicinity of the slots.

The measurement setup for measuring the radiation patterns of the tag antenna is shown in Figure 6. The proposed tag antenna is carried out in an anechoic chamber at the Korea RFID/USN Center, Incheon, and Republic of Korea. A range antenna used standard horn antenna and the tag antenna (AUT) was fixed to the receiving roll tower. Transmit and receive antennas were separated by a $10\lambda_0$ distance. Antenna measurement equipment were used Midas of ORBIT/FR and Anritsu vector network analyzer.

Figure 7 shows the measured radiation patterns with and without steel-bar. The proposed tag antenna was measured by attaching a steel-bar of 35 mm diameter and 200 mm length. It can be seen that the radiation patterns in the yz -plane and xz -plane are Z -axis directional for all frequencies. When the tag antenna attached in the steel-bar, the back-radiation decreased compared with the without steel-bar. In additional, the antenna gain was slightly decreased. The antenna is radiated towards the broadside with symmetrical radiation patterns in the E and H -planes.

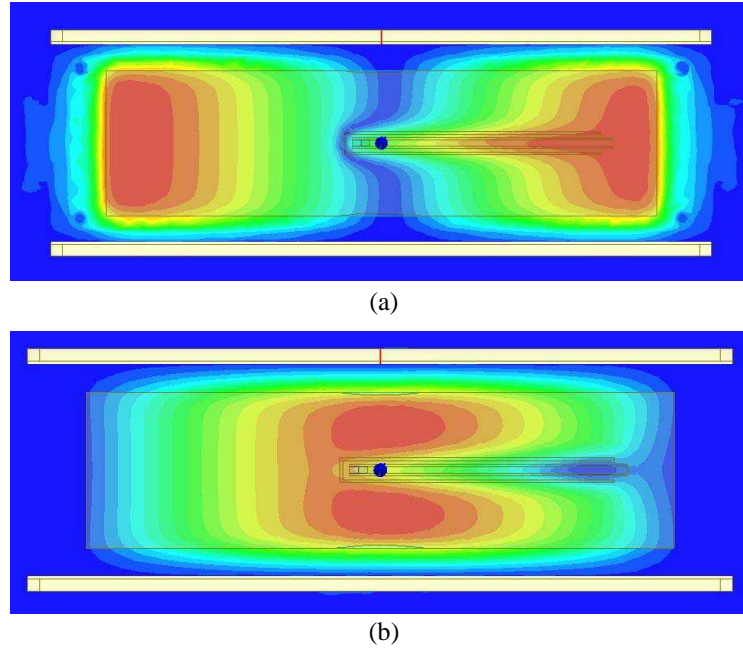


Figure 5. Simulated E and H field distribution at 920 MHz: (a) E -field and (b) H -field.

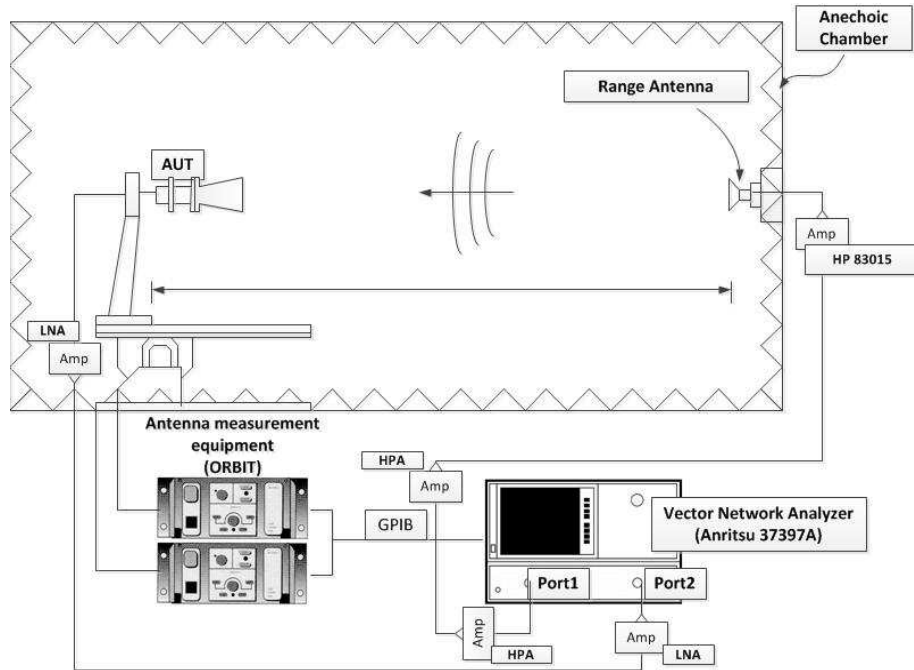


Figure 6. Set up environment of tag antenna radiation pattern.

Figure 8 shows the measured proposed antenna gains with and without steel-bar. The proposed tag antenna measured the gain at intervals of 10 MHz, and has the highest gain at the operating frequency band. When there was the steel-bar, it confirmed that gain value is dramatically decreased at the high frequency band. When there was no steel-bar, measured peak tag antenna gains of about 2.3 dBi at 902 MHz, 2.76 dBi at 920 MHz and 2.18 dBi at 928 MHz were obtained. When there was steel-bar, measured peak tag antenna gains of about 0.9 dBi at 902 MHz, 2.0 dBi at 920 MHz and 0.2 dBi at 928 MHz were obtained.

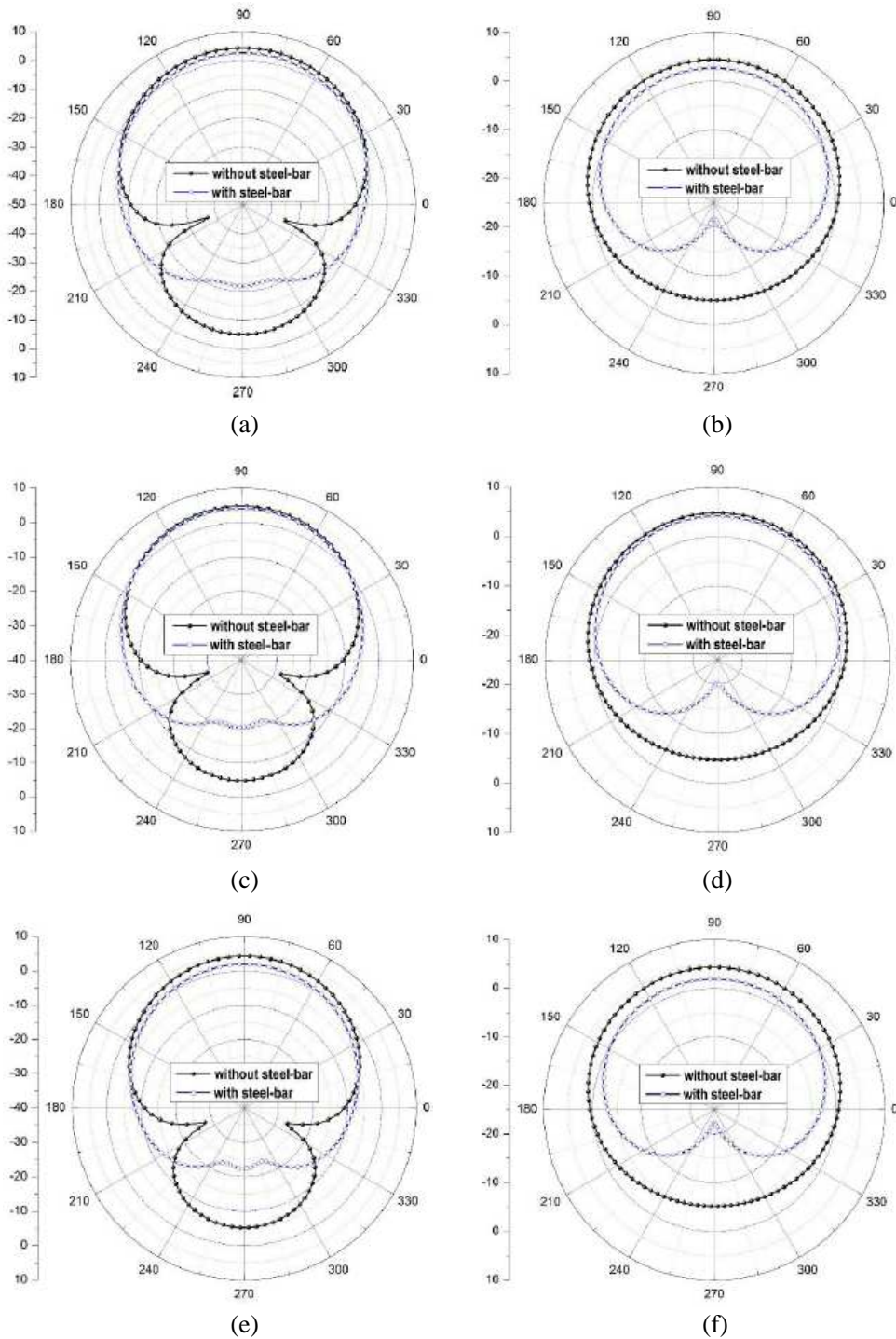


Figure 7. Measured radiation patterns: (a) yz -plane at 902 MHz, (b) xz -plane at 902 MHz, (c) yz -plane at 920 MHz, (d) xz -plane at 920 MHz, (e) yz -plane at 928 MHz, (f) xz -plane at 928 MHz.

Figure 9 shows the measurement setup for measuring the reading range of the tag antenna. In this experiment, based on the back-scattering method, the measurement of the tag antenna with the microchip (Alien Higgs-3 flip chip) is carried out in an anechoic chamber at the Korea RFID/USN Center, Incheon, Republic of Korea. The RFID reader used Alien reader and it transmits a wake-up signal to the proposed tag. The reference reader antenna used an LS AU-9007 which has a frequency

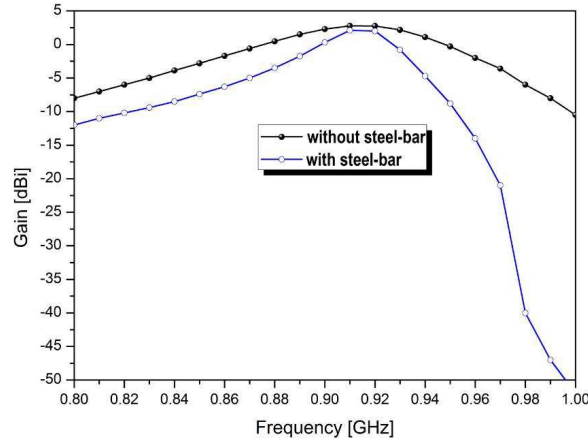


Figure 8. Measured antenna gains with and without steel-bar.

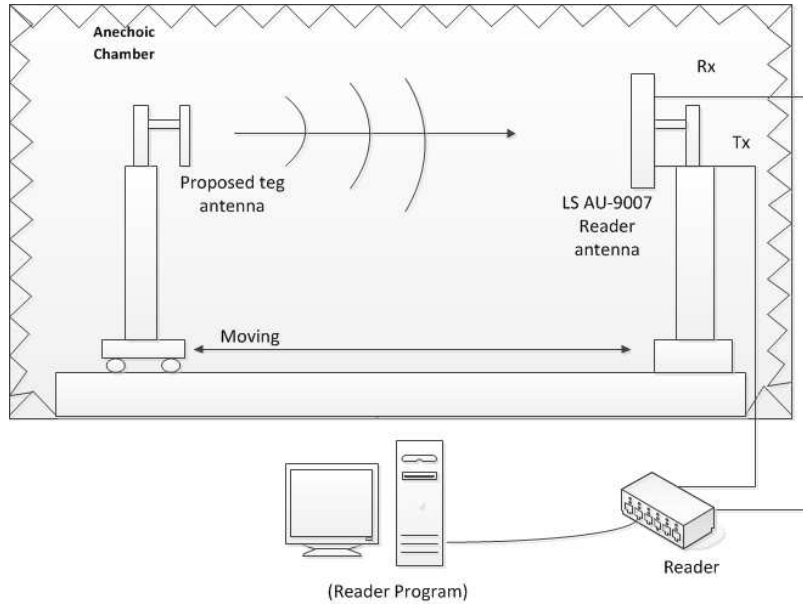


Figure 9. Setup environment of tag reading range.

range of 902 to 928 MHz and reader antenna gain is 6 dBi. The input power of the reader antenna is 1 W (30 dBm). The tag antenna gain used measured gain value of the Figure 8. The tag antenna is measured at an interval of ten seconds, and the proposed tag antenna automatically moves from 1 m to 20 m. The tag antenna is measured at the vertical position.

Figure 10 shows the calculation and measured tag antenna reading range. In this paper, the tag reading range is calculated based on [21]:

$$\text{reading range} = \frac{\lambda}{4} \sqrt{\frac{P_{\text{reader}} G_{\text{reader}} G_{\text{tag}}}{P_{c,\text{th}}}}$$

P_{reader} is 30 dBm, G_{reader} is 6 dBi, G_{tag} is from -52 to 2.78 dBi and $P_{c,\text{th}}$ is -18 dBm.

Experiments on the tag antenna were carried out in an anechoic chamber at the Korea RFID/USN Center. We can see that when calculating the reading range, the maximum distance was 11.0 m, but when measuring the reading range, the maximum distance was 11.5 m at 920 MHz.

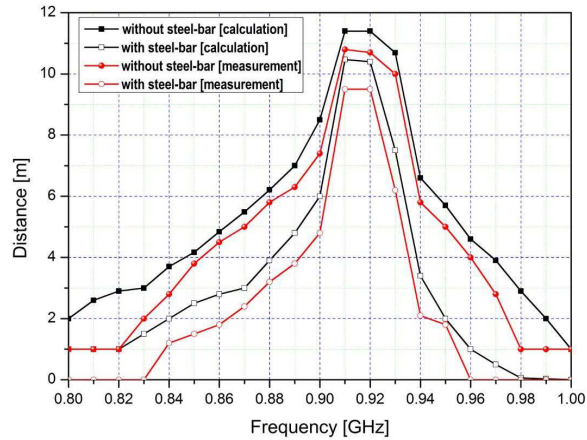


Figure 10. Measured and calculated reading ranges.

4. CONCLUSION

A UHF RFID slot coupled metallic tag antenna with a radome for steel-bar applications has been designed, fabricated, and tested. The proposed tag antenna can be easily frequency tuned by adjusting the antenna geometry and has very long reading range of 11.5 m on the metallic surface. The proposed metallic tag antenna can be used for UHF RFID communication applications.

ACKNOWLEDGMENT

This work was supported by the IT R&D program of MKE/KEIT. [10041628, Development of Radio Unit (RU) for multi-band, multi-RAT base stations, based on miniature modular RF units applicable to various cell environments of next generation cellular communications].

REFERENCES

1. Kim, J. D., et al., "Value analysis of location enabled radio-frequency identification information on delivery chain performance," *International Journal of Production Economics*, Vol. 112, No. 1, 403–415, 2008.
2. Kovavisaruch, L. O., P. Lertudomtana, and S. Horungruang, "Management truck tire information in logistic industry using RFID technology," *Portland International Center for Management of Engineering and Technology, Technology Management for a Sustainable Economy*, 1656–1665, 2008.
3. Wang, S. J., S. F. Liu, and W. L. Wang, "The simulated impact of RFID enabled supply chain on pull-based inventory replenishment in TFT-LCD industry," *International Journal of Production Economics*, Vol. 112, No. 2, 570–586, 2008.
4. Ke, X., et al., "Establishment of containers management system based on RFID technology," *International Conference on Computer Science and Software Engineering*, Vol. 6, 329–331, 2008.
5. Lee, J. N., et al., "Design of an ultra-compact UHF passive RFID tag antenna for a medical sample tube," *ETRI Journal*, Vol. 34, No. 6, 974–977, 2012.
6. Rahman, M. S., Y. G. Park, and K. D. Kim, "Relative location estimation of vehicles in parking management system," *International Conference on Advanced Communication Technology*, Vol. 3, 729–732, 2009.
7. Ali, K. and H. Hassanein, "Passive RFID for intelligent transportation systems," *IEEE Consumer Communications and Networking Conference*, 1–2, 2009.
8. Son, H. W., G. Y. Choi, and C. S. Pyo, "Design of wideband RFID tag antenna for metallic surfaces," *Electronics Letters*, Vol. 42, No. 5, 263–265, 2006.

9. Son, H. W. and G. Y. Choi, "Orthogonally proximity-coupled patch antenna for a passive RFID tag on metallic surfaces," *Microwave and Optical Technology Letters*, Vol. 49, No. 3, 715–717, 2007.
10. Son, H. W., "Design of RFID tag antenna for metallic surfaces using lossy substrate," *Electronics Letters*, Vol. 44, No. 12, 711–713, 2008.
11. Lin, D.-B., I.-T. Tang, and C.-C. Wang, "UHF RFID H-shaped tag antenna using microstrip feed design on metallic objects," *Journal of Electromagnetic Waves and Applications*, Vol. 25, No. 13, 1828–1839, 2011.
12. Lin, D.-B., C.-C. Wang, J.-H. Chou, and I.-T. Tang, "Novel UHF RFID loop antenna with interdigital coupled section on metallic objects," *Journal of Electromagnetic Waves and Applications*, Vol. 26, Nos. 2–3, 366–378, 2012.
13. Viani, F., M. Salucci, F. Robol, G. Oliveri, and A. Massa, "Design of a UHF RFID/GPS fractal antenna for logistics management," *Journal of Electromagnetic Waves and Applications*, Vol. 26, No. 4, 480–492, 2012.
14. Chen, S.-L., S.-K. Kuo, and C.-T. Lin, "A metallic RFID tag design for steel-bar and wire-rod management application in the steel industry," *Progress In Electromagnetics Research*, Vol. 91, 195–212, 2009.
15. Kim, J.-S., W.-K. Choi, and G.-Y. Choi, "Small proximity coupled ceramic patch antenna for UHF RFID tag mountable on metallic objects," *Progress In Electromagnetics Research C*, Vol. 4, 129–138, 2008.
16. Kim, J. W., et al., "Effects of a metal plane on a meandered slot antenna for UHF RFID applications," *Journal of Electromagnetic Engineering and Science*, Vol. 12, No. 2, 176–184, 2012.
17. Liu, Y., K.-M. Luk, and H.-C. Yin, "A RFID tag metal antenna on a compact his substrate," *Progress In Electromagnetics Research Letters*, Vol. 18, 51–59, 2010.
18. Ansoft, "High frequency structure simulator," HFSS Ver. 10, 2005.
19. Choi, W. K., et al., "RFID tag antenna coupled by shorted microstrip line for metallic surfaces," *ETRI Journal*, Vol. 30, No. 4, 597–599, 2008.
20. Nikitin, P. V., et al., "Sensitivity and impedance measurements of UHF RFID chips," *IEEE Transactions on Microwave Theory and Techniques*, Vol. 57, No. 5, 1297–1302, 2009.
21. Shepard, S., *RFID: Radio Frequency Identification*, McGraw-Hill, New York, 2005.